

Accepted Article

Title: Surface Modification of Two-Dimensional Metal-Organic Layers Creates Biomimetic Catalytic Microenvironments for Selective Oxidation

Authors: Wenjie Shi, Lingyun Cao, Hua Zhang, Xin Zhou, Bing An, Zekai Lin, Ruihan Dai, Jianfeng Li, Cheng Wang, and Wenbin Lin

This manuscript has been accepted after peer review and appears as an Accepted Article online prior to editing, proofing, and formal publication of the final Version of Record (VoR). This work is currently citable by using the Digital Object Identifier (DOI) given below. The VoR will be published online in Early View as soon as possible and may be different to this Accepted Article as a result of editing. Readers should obtain the VoR from the journal website shown below when it is published to ensure accuracy of information. The authors are responsible for the content of this Accepted Article.

To be cited as: *Angew. Chem. Int. Ed.* 10.1002/anie.201703675
Angew. Chem. 10.1002/ange.201703675

Link to VoR: <http://dx.doi.org/10.1002/anie.201703675>
<http://dx.doi.org/10.1002/ange.201703675>

Surface Modification of Two-Dimensional Metal-Organic Layers Creates Biomimetic Catalytic Microenvironments for Selective Oxidation

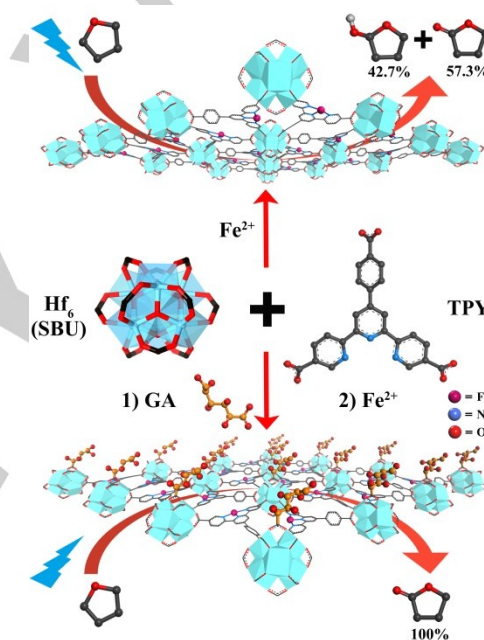
Wenjie Shi^[a], Lingyun Cao^[a], Hua Zhang^[a], Xin Zhou^[a,b], Bing An^[a], Zekai Lin^[c], Ruihan Dai^[a], Jianfeng Li^[a], Cheng Wang^{[a]*}, and Wenbin Lin^{[a,c]*}

Abstract: Microenvironments in enzymes play crucial roles in controlling the activities and selectivities of reaction centers. Herein we report the tuning of the catalytic microenvironments of metal-organic layers (MOLs), a two-dimensional version of metal-organic frameworks (MOFs) with thickness down to a monolayer, to control product selectivities. By modifying the secondary building units (SBUs) of MOLs with monocarboxylic acids such as gluconic acid, we successfully changed the hydrophobicity/hydrophilicity around the active sites and fine-tuned the selectivity in photocatalytic oxidation of tetrahydrofuran (THF) to exclusively afford butyrolactone (BTL), likely via prolonging residence time of reaction intermediates in the hydrophilic microenvironment of catalytic centers. Our work highlights new opportunities in using functional MOLs as highly tunable and selective two-dimensional catalytic materials.

Enzymes achieve high catalytic activities and selectivities under mild conditions by creating favorable microenvironments such as hydrophobic pockets around the reaction centers.^[1] For example, a number of oxidases achieve highly selective oxidative C-H functionalization in highly tailored reaction pockets using oxygen as the electron acceptor.^[2] Various artificial systems have been developed to mimic Nature's designs, ranging from cyclodextrin inclusion compounds^[3] and supramolecular cages^[4] to surface-decorated nanoparticles^[5] and porous Metal-Organic Frameworks (MOFs).^[6] However, reactions like selective oxidation of C-H bonds still present formidable challenges to synthetic chemists, in part due to the inability to precisely control the microenvironments in artificial catalysts.

Here we report Metal-Organic Layers (MOLs) as a new platform to rationally construct catalytic centers having rich secondary interactions with reaction intermediates for highly selective oxidations. MOLs are a two-dimensional version of Metal-Organic Frameworks (MOFs)^[7] with one dimension reduced to a monolayer in thickness.^[8] By replacing BTB in our previously reported $[\text{Hf}_6(\mu_3\text{-O})_4(\mu_3\text{-OH})_4(\text{HCO}_2)_6(\text{BTB})_2]$ MOLs (where BTB is benzenetribenzoate) with (4'-(4-benzoate)-(2,2',2''-terpyridine)-5,5''-dicarboxylate) (TPY), we obtained a new MOL of the composition $[\text{Hf}_6(\mu_3\text{-O})_4(\mu_3\text{-OH})_4(\text{HCO}_2)_6(\text{TPY})_2]$ with the TPY groups available for postsynthetic coordination of transition metal centers. Importantly, the six formate groups on the $[\text{Hf}_6(\mu_3\text{-O})_4(\mu_3\text{-OH})_4(\text{HCO}_2)_6]$ SBUs are pointing away from the nano-sheet and can be readily exchanged with functional

molecules with carboxylate anchoring groups, offering a convenient means to modify SBUs and alter the hydrophilic/hydrophobic environments of catalytic sites. By engineering Fe^{II} -tpy sites on the MOLs and the hydrophilic environment around them, we have designed a heterogeneous oxidase-mimicking catalyst for aerobic transformation of THF to butyrolactone (BTL) with 100% selectivity, a reaction of significant commercial interest.^[9] The selectivity can be tuned to afford different products by simply modifying the SBUs with various monocarboxylic acids (Scheme 1).



Scheme 1. Modifying the SBUs of Fe^{II} -MOLs with gluconic acid for the selective oxidation of tetrahydrofuran.

$[\text{Hf}_6(\mu_3\text{-O})_4(\mu_3\text{-OH})_4(\text{HCO}_2)_6(\text{TPY})_2]$ was prepared following the published procedure for $[\text{Hf}_6(\mu_3\text{-O})_4(\mu_3\text{-OH})_4(\text{HCO}_2)_6(\text{BTB})_2]$.^[8h] The MOLs appeared as wrinkled ultrathin films of ~ 0.2 μm in dimensions by Transmission Electron Microscopy (TEM) (Figure S1a & S2), and their Powder X-Ray Diffraction (PXRD) patterns were consistent with the 3,6-connected 2-D net of kgd topology (Figure 1a). The as-synthesized MOLs were measured to be 1.4 ± 0.2 nm in thickness by Atomic Force Microscopy (AFM), corresponding to the van der Waals diameter of a single layer of Hf_6 SBUs (Figure S1b&c). Fe^{II} centers were coordinated to the tpy sites by treating the MOLs with FeBr_2 , FeCl_2 , or $\text{Fe}(\text{OTf})_2$ (OTf = triflate) at room temperature for 24 hours. Inductively coupled plasma-optical emission spectroscopy (ICP-OES) gave an Fe loading of 10.35 wt%, indicating complete functionalization of the tpy sites. Fe^{II} -MOLs were light yellow with broad absorptions at < 350 nm and a tail extending to 420 nm, while the corresponding Fe^{III} -MOLs were purple in color with broad absorptions before 350

[a] W. Shi, L. Cao, H. Zhang, B. An, R. Dai, Prof. J. Li, Prof. C. Wang, Prof. W. Lin
College of Chemistry and Chemical Engineering, iCHEM, PCOSS
Xiamen University, Xiamen 361005 (China)
E-mail: wangchengxmu@xmu.edu.cn

[b] X. Zhou
School of Chemistry and Chemical Engineering, South China
University of Technology, Guangzhou 510640 (China)

[c] Z. Lin, Prof. W. Lin
Department of Chemistry, University of Chicago
Chicago, IL 60637 (USA)
E-Mail: wenbinlin@uchicago.edu

COMMUNICATION

WILEY-VCH

nm and a pronounced absorption band centered at ~370 nm (Figure 1b).

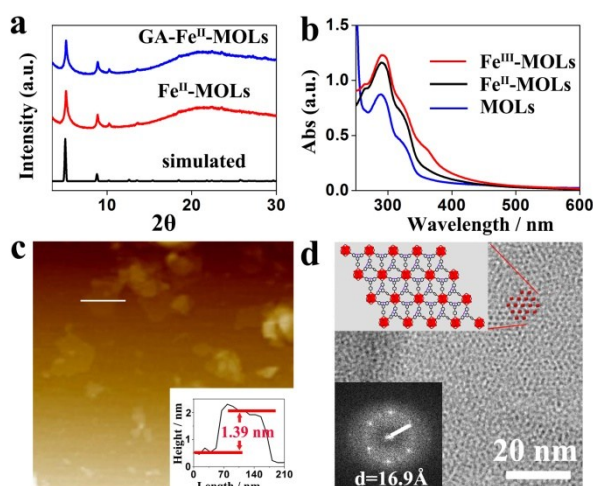


Figure 1. (a) PXRD patterns of GA-Fe^{II}-MOLs and Fe^{II}-MOLs. (b) UV-Vis spectra of MOLs (blue), Fe^{II}-MOLs (black), and Fe^{III}-MOLs (red). (c) Atomic force microscopy (AFM) image of GA-Fe^{II}-MOLs. (d) HRTEM and FFT images of GA-Fe^{II}-MOLs after catalysis.

The SBUs of Fe-MOLs were modified by treatment with different monocarboxylic acids in DMF at 60 °C for 24 hours (Figure S4&5). Eight monocarboxylic acids of varying hydrophilicity/hydrophobicity, including gluconic acid (GA), oleic acid (OA), caprylic acid (CA), propionic acid (PA), 5-aminovaleric acid (5-AA), 7-aminoheptanoic acid (7-AA), O-[2-(2-Methoxyethoxy)ethyl]glycolic acid (O-GA), and protoporphyrin IX (PPIX), were employed to tune the microenvironments around the tpy-Fe sites.

Thermogravimetric analysis (TGA) exhibited additional weight losses for MOLs treated with monocarboxylic acids, suggesting successful modification of the SBUs (Figure S3 and Table S1). For example, GA-MOLs exhibited an additional 8.4% weight loss as compared to the as-synthesized MOLs, consistent with the replacement of 16.7% of the capping formates by gluconates (*i.e.* one gluconate per SBU).

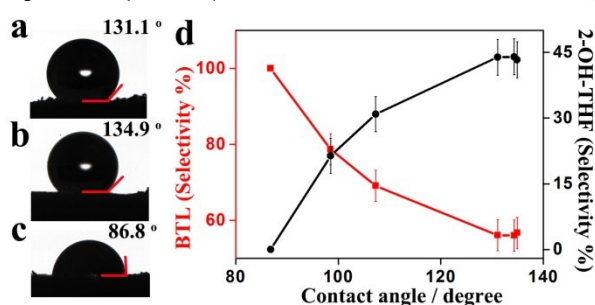


Figure 2. (a-c) Micrographs of water droplets on films of as-synthesized MOLs (a), OA-modified MOLs (OA-MOLs) (b), and GA-MOLs (c). (d) Relationship between BTL selectivity and MOL contact angles in aerobic oxidation of tetrahydrofuran. (Red: BTL selectivity; Black: 2-hydroxyl-tetrahydrofuran selectivity).

The unmodified MOLs were hydrophobic with a contact angle of $131.1^\circ \pm 0.5^\circ$ in water wettability test (Figure 2a). Upon modification with OA, the contact angle increased to $134.9^\circ \pm 0.5^\circ$, suggesting the creation of a more hydrophobic surface (Figure 2b). In contrast, after treating the MOLs with GA, the surface became hydrophilic with a contact angle of $86.8^\circ \pm 0.5^\circ$ (Figure 2c). TEM images and PXRD patterns of the modified samples indicated the preservation of the MOL structure after

SBU modifications (Figure 1a&d). AFM images of GA-Fe^{II}-MOLs gave a thickness of 1.4 ± 0.2 nm, similar to that of Fe^{II}-MOLs within experimental error (1.4 ± 0.2 nm; Figure 1c and Figure S1b&c).

The SBU modification of 2D-MOLs is more than a simple extension of postsynthetic functionalization of SBUs in 3D MOFs^[10]. First, there is no limitation on the size of monocarboxylate functional molecules due to the open space around a 2D net. Second, the position/geometry of modifying groups around catalytic sites can be easily controlled due to lower connectivity and complexity in 2D MOLs. Third, a high degree of SBU modification on MOLs can be achieved due to the absence of diffusion barriers. Furthermore, SBU functionalization of MOLs affords very different structures from surface modification of bulk MOFs: polymer-treated MOFs exhibited pre-concentration/gating effects in catalysis,^[6a,6c] while SBU modification in this work directly alters the microenvironment of reaction centers, allowing for significant enhancement of product selectivity.

We tested the catalytic activity of as-synthesized Fe^{II}-MOLs towards oxidative C-H activation of THF. Under the irradiation of a blue LED (~462 nm), 2 mg of Fe^{II}-MOLs was placed in a flask with 3 mL of aerated THF together with a catalytic amount (2 μ l) of acetic acid or formic acid. After 24 hours, the reaction mixture was analyzed by gas chromatography (GC) and GC-mass spectrometry (GC-MS). BTL and 2-hydroxyl-tetrahydrofuran (2-OH-THF) were two major products, with a BTL selectivity of 53.5 and a total turnover number (1/2 O₂-TON) of $(8.2 \pm 0.3) \times 10^2$ (Table 1, entry 1; Figure S8). Control experiments in the dark with or without heating at 50 °C showed negligible amount of products, confirming the photocatalytic nature of the reaction (Table 1, entries 2&3). The MOLs without Fe^{II} centers were inactive, indicating that tpy-Fe^{II} complex is the reaction center (Table S2, entry 1). We also found that O₂ and catalytic amount of acid (2 μ l) were essential for the oxidation of THF (Table 1, entry 4; Table S2, entries 2&3).

The heterogeneous nature of the MOL catalyst was proved by the lack of activity for the supernatant after removal of the MOL. TEM (Figure 1d) and PXRD studies confirmed that the GA-Fe^{II}-MOLs catalyst retained the same nanosheet structure after the catalytic reaction (Figure S7). A homogeneous control experiment using the tpy-Fe^{II} complex gave a low TON of 45 ± 2 , suggesting inter-molecular deactivation of the homogeneous catalysts in solution and highlighting the advantage of site-isolated MOL for efficient catalysis.

SBU modification greatly impacted the product selectivity of THF oxidation (Table 1, entries 5-12; Figure 2d). OA-Fe^{II}-MOLs with a hydrophobic surface gave a lower BTL selectivity of 56.7%, while the BTL selectivity increased to 78.7% for O-GA-Fe^{II}-MOLs with a less hydrophobic surface (Figure S6). Notably, the more hydrophilic GA-Fe^{II}-MOLs showed 100% selectivity for BTL with a TON of $(5.3 \pm 0.3) \times 10^2$. The relationship between BTL selectivities and MOL contact angles is shown in Figure 2d. In reactions with hydrophobic MOLs, we also observed the hydrolysis of some BTL (20%-40%) to the ring-opened product 4-hydroxyl-butanoic acid (Figures S8&S9).

We also explored the substrate scope of the MOL catalyst in oxidative activation of other C-H bonds. For example, tetrahydrofuran was also oxidized to oxotetrahydrofuran with a TON of 9.0 ± 0.3 under the photocatalytic conditions (Figure S10a). The MOLs functionalized with Fe(OTf)₂ oxidized cyclohexane with oxygen as the oxidant to form cyclohexanol and cyclohexanone in a 1:1 ratio with a TON of 4.0 ± 0.2 (Figure S10b).

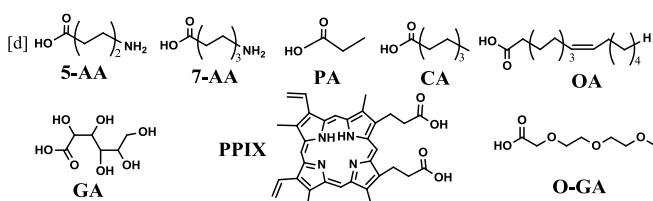
COMMUNICATION

WILEY-VCH

Table 1. Photocatalytic Oxidation of THF

Entry	Catalyst	Selectivity%		TON
		2-OH-THF	BTL	
1	Fe ^{II} -MOLs	43 ± 4	57 ± 4	(8.2 ± 0.3) × 10 ²
2	Fe ^{II} -MOLs ^[a]	-	-	2.0 ± 0.1
3	Fe ^{II} -MOLs ^[b]	-	-	5.0 ± 0.2
4	Fe ^{II} -MOLs ^[c]	-	-	4.0 ± 0.2
5	GA-Fe ^{II} -MOLs ^[d]	0	100	(5.3 ± 0.3) × 10 ²
6	O-GA-Fe ^{II} -MOLs	21 ± 4	79 ± 4	(6.8 ± 0.3) × 10 ²
7	PPIX-Fe ^{II} -MOLs	31 ± 4	69 ± 4	(5.9 ± 0.3) × 10 ²
8	OA-Fe ^{II} -MOLs	43 ± 4	57 ± 4	(7.8 ± 0.3) × 10 ²
9	CA-Fe ^{II} -MOLs	44 ± 4	56 ± 4	(9.3 ± 0.3) × 10 ²
10	PA-Fe ^{II} -MOLs	42 ± 4	58 ± 4	(8.8 ± 0.3) × 10 ²
11	5-AA-Fe ^{II} -MOLs	44 ± 4	56 ± 4	(7.2 ± 0.3) × 10 ²
12	7-AA-Fe ^{II} -MOLs	44 ± 4	56 ± 4	(7.8 ± 0.3) × 10 ²

[a] Without light. [b] Heating at 50 °C without light. [c] Without oxygen.



We studied the mechanism of the photocatalytic aerobic THF oxidation.

Singlet oxygen was first ruled out as the oxidant, since Ru(bpy)₃²⁺, which is known to generate singlet oxygen,^[11] did not oxidize THF under the photocatalytic conditions.

The reaction is also unlikely to proceed via hydroxyl or hydroperoxyl free radicals from activated oxygen. The Fenton's reagent FeSO₄/H₂O₂ that generated these radicals, oxidized THF to a complex mixture of oxirane (4%), oxetane (3%), 2-OH-THF (8%), 2-hydroperoxyl-tetrahydrofuran (11%), 1,4-butan-diol (17%), BTL (43%), 4-hydroxyl-butanoic acid (3%) and other unidentified species (11%) (Figure S9), in contrast to the high selectivity towards BTL and 2-OH-THF by the MOLs (Figure S8). Consistent with the absence of free radical involvement, adding 5,5-dimethyl-1-pyrroline-N-oxide (DMPO) as a radical trapping agent (80 mM) in the reaction failed to produce DMPO adducts with either hydroxyl or hydroperoxyl radicals as shown by electron spin resonance (ESR) spectroscopy.

We proposed a catalytic cycle as shown in Scheme 2a. The tpy-Fe^{II} (**1**) is oxidized to tpy-Fe^{III} (**2**) by oxygen in the presence of protons, followed by photochemical oxidation of THF by tpy-Fe^{III}-OOH.

The generation of Fe^{III} species is confirmed by the X-band ESR spectroscopy. The starting high-spin tpy-Fe^{II} complex was ESR silent with S=2 (Figure 3a) and was confirmed by X-ray photoelectron spectroscopy (Figure S7c). In the presence of both acid and oxygen, a THF suspension of the Fe-MOLs in the dark at 90 K showed a rhombic ESR spectrum with g=6.17, g=4.23 and g=1.93, typical of high-spin Fe^{III} centers with S=5/2 (Figure 3a; Figure S11).^[12] In the absence of acid or air, no ESR signal was detected with or without light irradiation. These results also suggest that light is not needed in the generation of Fe^{III}, consistent with the observation of the reaction mixture turning purple to form tpy-Fe^{III} in the absence of light.

We hypothesize that the Fe^{III} was generated by proton-coupled electron transfer (PCET) from the Fe^{II} center to a coordinated O₂. DFT calculations supported this PCET process, as spin and orbital analysis showed an Fe^{II} center for tpy-Fe-O₂

adducts but an Fe^{III} center for the tpy-Fe-OOH complex (see SI section 10). The ν(O-O) vibration in Fe^{III}-OOH was observed at 1021 cm⁻¹ in the Raman spectrum (Figure 3b), as expected for a protonated superoxide.^[13]

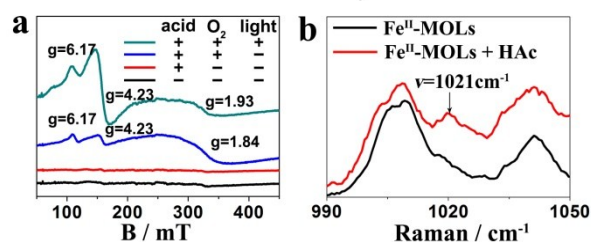


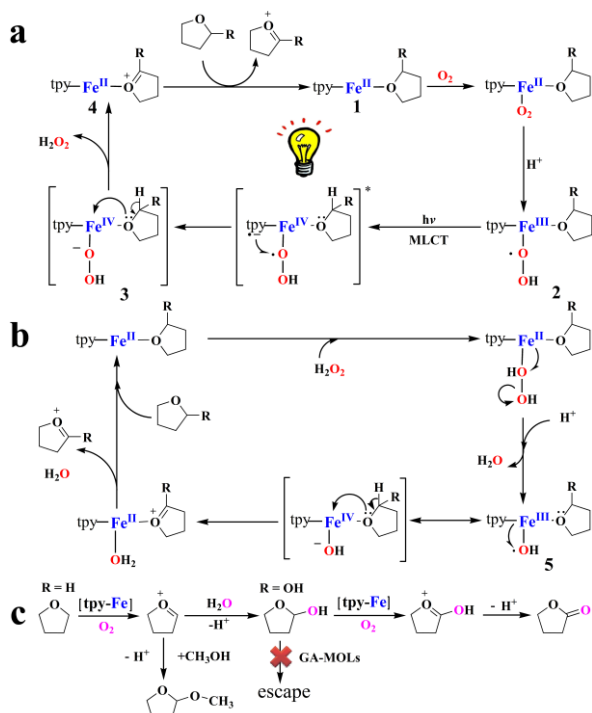
Figure 3. (a) ESR spectra of Fe^{II}-MOLs in THF at 90K (black), with acetic acid but without oxygen (red), with acetic acid and oxygen in dark (blue) and after irradiation with blue light (cyan). (b) Raman spectra of Fe^{II}-MOLs (black) with acetic acid and Fe^{II}-MOLs (red) in THF.

The second step in the cycle involves photochemical oxidation of THF by tpy-Fe^{III}-OOH. In the MLCT excited state of tpy-Fe^{III}-OOH, i.e. tpy⁻-Fe^{IV}-OOH, the tpy⁻ radical anion transfers one electron to Fe^{IV}-OOH to generate tpy-Fe^{IV}-OOH (**3**). The Fe^{IV} center oxidizes coordinated THF via a two-electron transfer to form Fe^{II}-coordinated oxonium cation (**4**), which is attacked by water to generate 2-OH-THF. The oxonium as an intermediate was supported by the exclusive formation of 2-methoxyl-tetrahydrofuran when methanol was added to the reaction mixture. H₂O₂ can also be produced in the process, as corroborated by electrochemical detection of H₂O₂ with a Faraday efficiency of 97% on a rotating ring-disk electrode using Fe^{II}-MOLs as the oxygen reduction electrocatalyst (Figure S12).

The tpy-Fe^{II} species can also react with the generated H₂O₂ in a Fenton-like process to generate tpy-Fe^{III}-OH adduct (**5**, in resonance to tpy-Fe^{IV}-OH) that oxidizes THF to oxonium cation via two-electron transfer (Scheme 2b). The much higher redox potential of [•]OH/[•]OH (1.90 V vs. SHE) than that of [•]OOH/[•]OOH (0.75 V vs. SHE)^[14] enables direct oxidation of Fe^{III} to Fe^{IV} in the absence of photo-excitation. We confirmed in control experiments that H₂O₂ can oxidize THF in dark with Fe^{II}-MOLs as the catalyst [TON = (8.8 ± 0.3) × 10² in 24 hours].

The 2-OH-THF from THF oxidation can also be adsorbed onto the Fe centers and further oxidized by both the tpy⁻-Fe^{IV}-OOH and tpy-Fe^{IV}-OH to form BTL (Scheme 2c), as confirmed by using 2-OH-THF as the substrate in the aerobic photo-oxidation with a TON of (6.3 ± 0.3) × 10² in 24 hours.

To identify the rate-determining step in this catalytic cycle, the H/D kinetic isotope effect (KIE) for THF oxidation was measured using C₄H₈O and C₄D₈O as the substrates in two separate experiments. The resulting KIE values are 1.3 ± 0.2 for 2-OH-THF and 1.2 ± 0.2 for BTL, suggesting only secondary isotopic effect. In a related experiment using H₂O₂ as the oxidant in dark, the KIE values are 3.0 ± 0.2 for 2-OH-THF and 2.4 ± 0.2 for BTL, which are typical values for primary kinetic isotope effect. The absence of the primary KIE in the photocatalysis and its presence in the dark reaction suggest the step after light activation as the rate-determining step (RDS) in the photocatalysis, possibly the step of electron transfer from tpy⁻ to [•]OOH. This assignment of RDS is also consistent with the ESR observation of Fe^{III} species as the catalyst resting state, which is the state before light activation. We have also added D₂O and H₂O into the reaction mixtures without observing any rate differences in THF oxidation, confirming that the protonation of adsorbed oxygen on Fe^{II} or the addition of water to oxonium is not the rate-determining step.



Scheme 2. Proposed catalytic cycle of (a) O_2 -dependent and (b) H_2O_2 -dependent reactions for the oxidation of THF and 2-OH-THF. c) Conversion of THF to 2-OH-THF and BTL.

With this catalytic cycle, we can rationalize the effects of microenvironments on reactivity by retaining 2-OH-THF in hydrophilic pockets, which leads to subsequent oxidation of 2-OH-THF to BTL. We measured the uptake of 2-OH-THF by MOLs with different modifications via equilibrating 23 mM of the adsorbates with 3.4 mM of MOLs followed by determining the adsorbate concentration in the supernatant by GC-MS.^[6b] The 2-OH-THF uptake was 0 for as-synthesized MOLs, 0 for hydrophobic CA-MOLs and 1.18 mol/mol MOLs for hydrophilic GA-MOLs, supporting the retention of 2-OH-THF in hydrophilic microenvironment.

In summary, we developed a method to modify the SBUs of catalytic metal-organic layers with monocarboxylate compounds, which creates hydrophilic/hydrophobic microenvironments around the reaction centers and controls the selectivity in the photocatalytic aerobic oxidation of THF. This assembly mimics oxidase in using secondary interactions to direct reaction pathways, and highlights opportunities in using functionalized metal-organic layers in biomimetic catalysis.

Acknowledgements

We acknowledge funding support from the National Natural Science Foundation and Ministry of Science and Technology of the P.R.China (NSFC21671162, 2016YFA0200702, NSFC21471126), the National Thousand Talents Program of the P. R. China, Post-Doctoral Innovative Talents Project (BX201600053) from China Postdoctoral Science Foundation and the U.S. National Science Foundation (DMR-1308229).

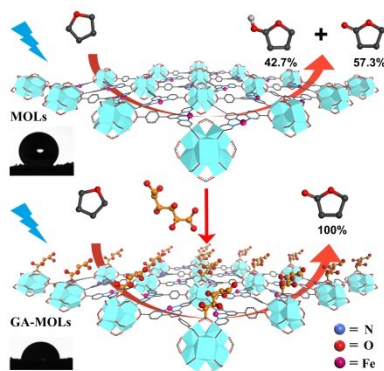
Keywords: Metal-Organic Layers; Metal-Organic Frameworks; microenvironment; biomimetic; photocatalysis

Reference

- [1] A. White, *Principles of biochemistry* A. White, P. Handler and E. L. Smith, Blakiston Division, McGraw-Hill, New York, **1968**.
- [2] a) F. Hollmann, I. W. C. E. Arends, K. Buehler, A. Schallmeyer, B. Buhler, *Green Chem.* **2011**, *13*, 226-265; b) R. Fasan, *ACS Catal.* **2012**, *2*, 647-666.
- [3] a) A. Hashidzume, H. Yamaguchi, A. Harada, *Acc. Chem. Res.* **2014**, *34*, 71-110; b) E. Lindbäck, Y. Zhou, C. M. Pedersen, M. Bols, *Tetrahedron Lett.* **2012**, *53*, 5023-5026; c) Y. Yang, Y. Sun, N. Song, *Acc. Chem. Res.* **2014**, *47*, 1950-1960.
- [4] a) D. M. Kaphan, M. D. Levin, R. G. Bergman, K. N. Raymond, F. D. Toste, *Science* **2015**, *350*, 1235-1238; b) Y. Inokuma, M. Kawano, M. Fujita, *Nat Chem* **2011**, *3*, 349-358.
- [5] a) Y. Dai, S. Liu, N. Zheng, *J. Am. Chem. Soc.* **2014**, *136*, 5583-5586; b) J. Gao, X. Zhang, Y. Yang, J. Ke, X. Li, Y. Zhang, F. Tan, J. Chen, X. Quan, *Chem. - Asian J.* **2013**, *8*, 934-938; c) H. Wei, E. Wang, *Chem. Soc. Rev.* **2013**, *42*, 6060-6093; d) C. Yuan, W. Luo, L. Zhong, H. Deng, J. Liu, Y. Xu, L. Dai, *Angew. Chem., Int. Ed.* **2011**, *50*, 3515-3519; *Angew. Chem.*, **2011**, *123*, 3577-3581.
- [6] a) Z. Zhang, H. T. H. Nguyen, S. A. Miller, A. M. Ploskonka, J. B. Decoste, S. M. Cohen, *J. Am. Chem. Soc.* **2016**, *138*, 920-925; b) D. J. Xiao, J. Oktawiec, P. J. Milner, J. R. Long, *J. Am. Chem. Soc.* **2016**, *138*, 14371-14379; c) G. Huang, Q. Yang, Q. Xu, S.-H. Yu, H.-L. Jiang, *Angew. Chem., Int. Ed.* **2016**, *55*, 7379-7383; *Angew. Chem.* **2016**, *128*, 7505; d) M. Zhao, S. Ou, C. Wu, *Acc. Chem. Res.* **2014**, *47*, 1199-1207; e) D. Feng, Z. Gu, J. Li, H. Jiang, Z. Wei, H. Zhou, *Angew. Chem. Int. Ed.* **2012**, *51*, 10307-10310; *Angew. Chem.* **2012**, *124*, 10453-10456; f) K. P. Lillerud, U. Olsbye, M. Tilset, *Top. Catal.* **2010**, *53*, 859-868; g) T. Kajiwara, M. Fujii, M. Tsujimoto, K. Kobayashi, M. Higuchi, K. Tanaka, S. Kitagawa, *Angew. Chem., Int. Ed.* **2016**, *55*, 2697-2700; *Angew. Chem.* **2016**, *128*, 2747; h) P. Wu, C. He, J. Wang, X. Peng, X. Li, Y. An, C. Duan, *J. Am. Chem. Soc.* **2012**, *134*, 14991-14999. i) Z. Hu, D. Zhao, *CrystEngComm* **2017**. doi: 10.1039/C6CE02660E.
- [7] a) H. Furukawa, K. E. Cordova, M. O. Keeffe, O. M. Yaghi, *Science* **2013**, *341*, 1230444-1230444; b) T. Devic, P. Horcajada, C. Serre, F. Salles, G. Maurin, B. Moulin, D. Heurtaux, G. Clet, A. Vimont, J. M. Greneche, O. B. Le, M. Florian, M. Emmanuel, F. Yaroslav, L. J. C. D. Marco, G. Ferey, *J. Am. Chem. Soc.* **2010**, *132*, 1127-1136; c) T. L. Easun, F. Moreau, Y. Yan, S. Yang, M. Schroder, *Chem. Soc. Rev.* **2017**, *46*, 239-274; d) J. H. Cavka, S. Jakobsen, U. Olsbye, N. Guillou, C. Lamberti, S. Bordiga, K. P. Lillerud, *J. Am. Chem. Soc.* **2008**, *130*, 13850-13851; e) J. Lee, O. K. Farha, J. Roberts, K. A. Scheidt, S. T. Nguyen, J. T. Hupp, *Chem. Soc. Rev.* **2009**, *38*, 1450-1459.
- [8] a) P.-Z. Li, Y. Maeda, Q. Xu, *Chem. Commun.* **2011**, *47*, 8436-8438; b) S. Stepanow, N. Lin, D. Payer, U. Schlickum, F. Klappenberger, G. Zoppellaro, M. Ruben, H. Brune, J. V. Barth, K. Kern, *Angew. Chem., Int. Ed.* **2007**, *46*, 710-713; *Angew. Chem.*, **2007**, *119*, 724-727; c) A. Bétard, R. A. Fischer, *Chem. Rev.* **2012**, *112*, 1055-1083; d) T. Bauer, Z. Zheng, A. Renn, R. Enning, A. Stemmer, J. Sakamoto, A. D. Schlüter, *Angew. Chem., Int. Ed.* **2011**, *50*, 7879-7884; *Angew. Chem.*, **2011**, *123*, 8025-8030; e) M. G. Campbell, S. F. Liu, T. M. Swager, M. Dincă, *J. Am. Chem. Soc.* **2015**, *137*, 13780-13783; f) R. Dong, M. Pfeiffermann, H. Liang, Z. Zheng, X. Zhu, J. Zhang, X. Feng, *Angew. Chem., Int. Ed.* **2015**, *54*, 12058-12063; *Angew. Chem.*, **2015**, *127*, 12226-12231; g) Y. Peng, Y. Li, Y. Ban, H. Jin, W. Jiao, X. Liu, W. Yang, *Science* **2014**, *346*, 1356-1359; h) L. Cao, Z. Lin, F. Peng, W. Wang, R. Huang, C. Wang, J. Yan, J. Liang, Z. Zhang, T. Zhang, L. Long, J. Sun, W. Lin, *Angew. Chem., Int. Ed.* **2016**, *55*, 4962-4966; *Angew. Chem.* **2016**, *128*, 5046; i) Z. Hu, E. M. Mahdi, Y. Peng, Y. Qian, B. Zhang, N. Yan, D. Yuan, J.-C. Tan, D. Zhao, *J. Mater. Chem. A* **2017**. doi: 10.1039/C7TA00413C.
- [9] a) P. Padmalatha, P. K. Khatri, S. L. Jain, *Synlett* **2013**, *24*, 1405-1409; b) A. Ausavasukhi, T. Sooknoi, *Green Chem.* **2015**, *17*, 435-441.
- [10] a) J. S. Seo, D. Whang, H. Lee, S. I. Jun, J. Oh, Y. J. Jeon, K. Kim, *Nature* **2000**, *404*, 982-986; b) Z. Wang, S. M. Cohen, *Chem. Soc. Rev.* **2009**, *38*, 1315-1329.
- [11] A. A. Abdel-Shafi, H. A. Hassanin, S. S. Al-Shihry, *Photochem. Photobiol. Sci.* **2014**, *13*, 1330-1337.
- [12] G. Villar-Acevedo, E. Nam, S. Fitch, J. Benedict, J. Freudenthal, W. Kaminsky, J. A. Kovacs, *J. Am. Chem. Soc.* **2011**, *133*, 1419-1427.
- [13] B. S. Yeo, S. L. Klaus, P. N. Ross, R. A. Mathies, A. T. Bell, *ChemPhysChem* **2010**, *11*, 1854-1857.
- [14] C. Adriaanse, J. Cheng, V. Chau, M. Sulpizi, J. VandeVondele, M. Sprik, *The J. of Phys. Chem. Lett.* **2012**, *3*, 3411-3415.

Biomimetic catalysis

Two dimensional metal-organic-layers (MOLs) with Fe^{II} catalytic centers mimic oxidase in aerobic photo-oxidation of tetrahydrofuran. The product selectivity is fine-tuned through hydrophilic/hydrophobic modification of the MOLs, akin to the creation of suitable microenvironments in enzymes for selective catalysis.



Wenjie Shi, Lingyun Cao, Hua Zhang,
Xin Zhou, Bing An, Zekai Lin, Ruihan
Dai, Jianfeng Li, Cheng Wang*, and
Wenbin Lin*

Page No. – Page No.

Surface Modification of Two-
Dimensional Metal-Organic Layers
Creates Biomimetic Catalytic
Microenvironments for Selective
Oxidation